Food Chemistry: X 21 (2024) 101159

Contents lists available at ScienceDirect

Food Chemistry: X

journal homepage: www.sciencedirect.com/journal/food-chemistry-x

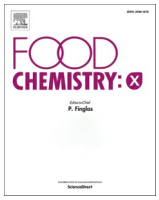

Comprehensive widely targeted metabolomics to decipher the molecular mechanisms of *Dioscorea opposita* thunb. cv. Tiegun quality formation during harvest

Li An [a,1], Yongliang Yuan [b,1], He Chen [a], Meng Li [a], Jingwei Ma [a], Juan Zhou [a], Lufei Zheng [c], Huan Ma [a], Zenglong Chen [d,*], Chenyu Hao [e], Xujin Wu [a,*]

[a] *Institute of Quality and Safety for Agro-products, Henan Academy of Agricultural Sciences, Key Laboratory of Grain Quality and Safety and Testing Henan Province, Zhengzhou 450002, China*
[b] *Department of Pharmacy, The First Affiliated Hospital of Zhengzhou University, Zhengzhou 450052, China*
[c] *Institute of Quality Standards and Testing Technology for Agro-products of CAAS, Beijing 100081, China*
[d] *State Key Laboratory of Integrated Management of Pest Insects and Rodents, Institute of Zoology, Chinese Academy of Sciences, Beijing 100101, China*
[e] *School of Public Health, Tianjin University of Traditional Chinese Medicine, Tianjin 301617, China*

ARTICLE INFO

Keywords:
Dioscorea opposita Thunb. cv. Tiegun
Widely targeted metabolomics
Metabolic changes
Harvest stage
Molecular mechanisms

ABSTRACT

Dioscorea opposita Thumb. cv. Tiegun is commonly consumed as both food and traditional Chinese medicine, which has a history of more than two thousand years. Harvest time directly affects its quality, but few studies have focused on metabolic changes during the harvesting process. Here, a comprehensive metabolomics approach was performed to determine the metabolic profiles during six harvest stages. Thirty eight metabolites with significant differences were determined as crucial participants. Related metabolic pathways including phenylalanine, tyrosine and tryptophan biosynthesis, stilbenoid, diarylheptanoid and gingerol biosynthesis, phenylpropanoid biosynthesis, flavonoid biosynthesis and tryptophan metabolism were the most active pathways during harvest. The results revealed that temperature has a significant impact on quality formation, which suggested that *Dioscorea opposita* thumb. cv. Tiegun harvested after frost had higher potential value of traditional Chinese medicine. This finding not only offered valuable guidance for yam production, but also provided essential information for assessing its quality.

1. Introduction

Yam, belonging to the Dioscorea genus, is a plant with the underground tuber as its main edible part. It is widely recognized as a tuber vegetable in Asia, America and Africa. In particular, China has a rich history of cultivating yam for thousands of years, where it has been utilized as both a food source and traditional medicine (Kawasaki, Kanehira & Islam, 2014; Epping & Laibach, 2020). The county of Wen in Jiaozuo city, located in Henan Province, serves as the primary production area, which is renowned for its high-quality yam products. Among the varieties, *Dioscorea opposita* thumb. cv. Tiegun, also known as "Tiegun Shanyao" in China, is particularly favored due to its exceptional nutritional and pharmaceutical value (Zhang, Gao, Wang & Huang, 2014). Over the course of two millennia, it has been employed in treating various ailments, including diarrhea, diabetes, and asthma (Epping & Laibach, 2020). *Dioscorea opposita* thumb. cv. Tiegun is abundant in nutritional and functional ingredients, including starch, protein, amino acids, polysaccharides, batatasins, allantoin, flavonoids, polyphenols and other bioactive compounds. These constituents exhibit essential pharmacological effects such as nourishing the spleen and stomach, anti-oxidation, anti-inflammation, regulation of gut microbiota, gastrointestinal protection, and anti-tumor properties (Li et al., 2023). Additionally, *Dioscorea opposita* thumb. cv. Tiegun also contains various bioactive secondary metabolites, which likely contribute to its use in traditional Chinese medicine and modern herbal remedies (Li et al., 2023). These secondary metabolites serve as the material basis for its clinically curative effects and are crucial indicators for evaluating the quality. For medicinal and edible homologous plants with roots and

* Corresponding authors.
E-mail addresses: chenzenglong@ioz.ac.cn (Z. Chen), xujinwu2005@126.com (X. Wu).
[1] Both authors contributed equally to this work and are co-first authors.

https://doi.org/10.1016/j.fochx.2024.101159
Received 13 November 2023; Received in revised form 19 January 2024; Accepted 21 January 2024
Available online 1 February 2024

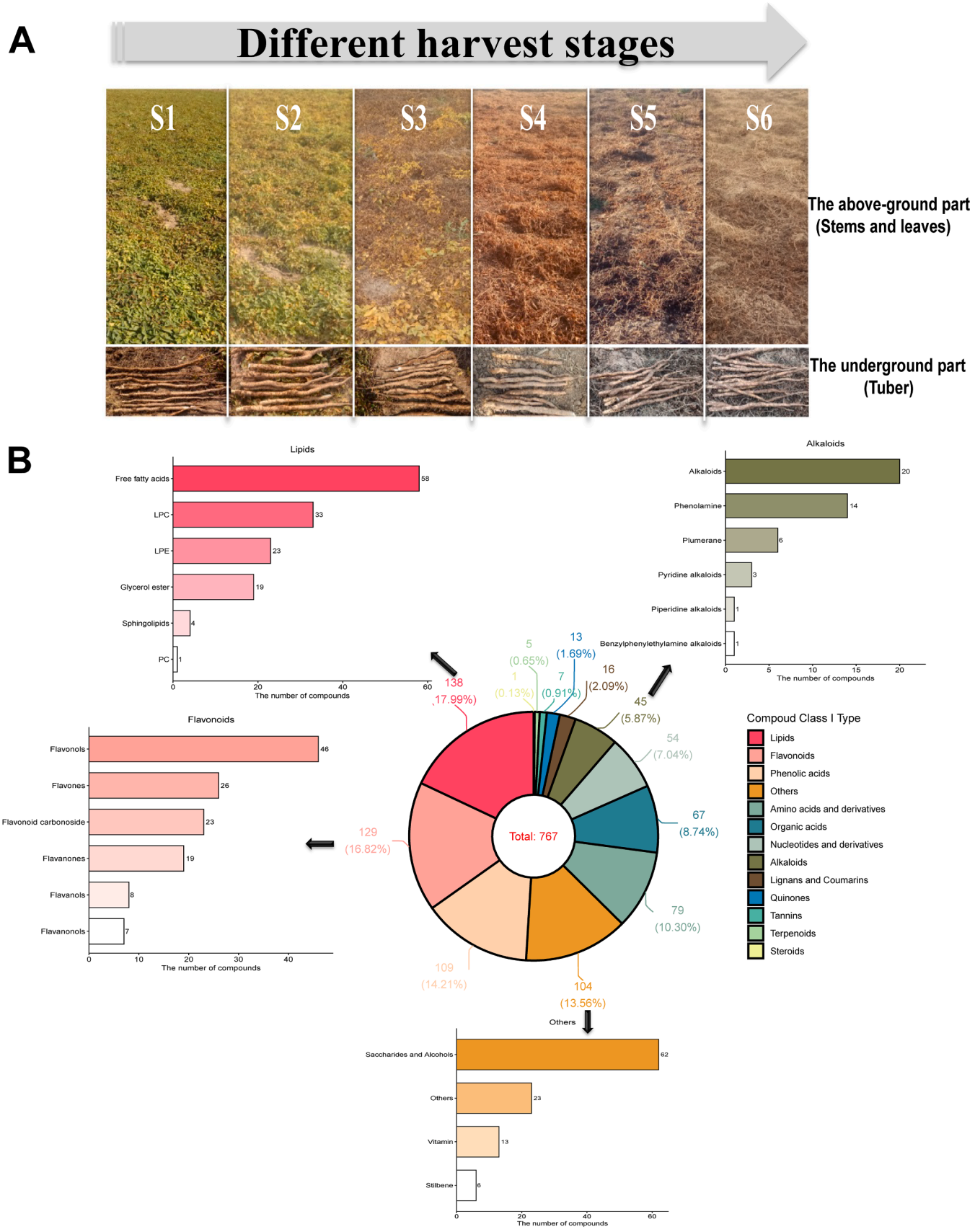

Fig. 1. Sample collection for six different harvest stages of *Dioscorea opposita* Thunb. cv. Tiegun (A), and types and proportions of identified metabolites (B).

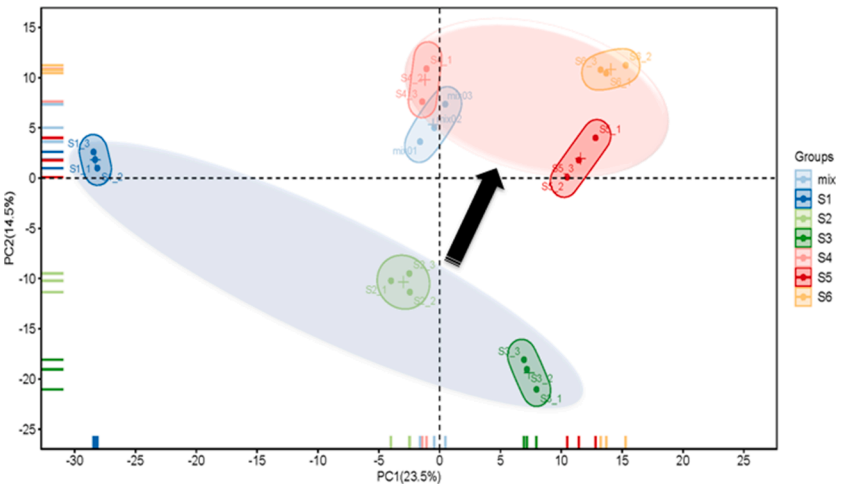

Fig. 2. PCA score plot for discrimination of 18 *Dioscorea opposita* Thunb. cv. Tiegun samples.

stems, the accumulation of active components is primarily influenced by the growth period (Li, Kong, Fu, Sussman & Wu, 2020). Thus, determining the optimal harvest time is crucial for obtaining optimal quality. However, previous studies have mainly focused on extraction techniques, bioactivities, detection methods and chemopreventive effects (Li et al., 2023; Li, Kong, Fu, Sussman & Wu, 2020). Systematic metabolic changes at different harvest stages and the molecular mechanisms of quality formation during harvest remain unclear.

Metabolomics has emerged as a powerful tool to acquire qualitative and quantitative information on low-molecular-weight metabolites of living organisms and biological samples, which enables comprehensive characterization of global metabolite changes, identification of differential metabolites that play essential roles, and preliminary exploration of the underlying causes for these changes. Widely targeted metabolomics, a novel technique, combines the generality of untargeted metabolomics and the accuracy of targeted metabolomics, which has high throughput, ultra-sensitivity, and wide coverage. This approach has found gradually application in food research, such as phytochemistry (Xue et al., 2022), stress tolerance (Zhang, Shen, Cao, Duan & Sun, 2023), geographical origin (Zhao et al., 2022), quality formation (Zhou et al., 2022; Zhang, Shen, Cao, Duan & Sun, 2023), and other areas. Determining the optimal harvest period is a critical factor in obtaining high-quality agricultural products. Recent studies have reported the influence of harvest time on plant quality using widely targeted metabolomics approaches. For instance, Deiana et al. evaluated the chemical composition of Italian virgin olive oils as a function of harvest period and cultivar, which provided guidelines for optimizing the timing of the harvesting process for olive oil producers (Deiana, Santona, Dettori, Culeddu, Dore & Molinu, 2019). Si et al. investigated the main metabolites in Dendrobium officinale leaves during the harvesting period and identified the most appropriate timing of collection during harvest (Si et al., 2022). However, no reports are available regarding the metabolic profiling of *Dioscorea opposita* thumb. cv. Tiegun during harvest.

Here, we attempt to utilize widely targeted metabolomics approach to comprehensively profile the metabolites of *Dioscorea opposita* thumb. cv. Tiegun during different harvest stages. The objective of this study is to determine the chemical component accumulation process and explore the underlying molecular mechanisms that contribute to quality formation.

2. Materials and methods

2.1. Plant samples collection

Dioscorea opposita thunb. cv. Tiegun was cultivated in Wen country, Henan Province, China (35°0′34″ N; 113°5′10″ E). Six different harvest stages samples were collected, respectively in September 23, Stage 1 (S1); October 10, Stage 2 (S2); October 23, Stage 3 (S3); November 10, Stage 4 (S4); November 23, Stage 5 (S5) and December 10, Stage 6 (S6).

2.2. Sample preparation and extraction

All collected samples were undamaged, which were cleaned with distilled water, air-dried, cut into 2 mm thick pieces, flash-frozen in liquid nitrogen, freeze-dried, powdered, and subsequently stored at −80 °C until analysis. Each sample from the distinct harvest periods included three replicates, with each replicate comprising five individual *Dioscorea opposita* Thunb. cv. Tiegun samples. Quality control (QC) samples were created by combining samples from each harvest stage. The extraction procedure followed the previously reported method by Zeng et al. (2021). 100 mg of the powder was extracted with 1.2 mL of 70 % aqueous methanol. The mixture was vortexed for 30 s at 30-minute intervals, repeating this process six times. The sample was then centrifuged at 12,000 rpm for 10 min at 4 °C. The resultant supernatant was finally filtered using a 0.22 μm filter and used for LC-MS/MS analysis.

2.3. Data processing

Samples were analyzed using a Shimadzu UHPLC 30A system equipped with Agilent SB-C18 (1.8 μm, 2.1 mm × 100 mm) column maintained at 40 °C. Based on methods described in the literature (Zeng, Liu & Huang, 2021), we performed method optimization. Gradient elution was performed with 0.1 % formic acid in water (solvent A) and 0.1 % formic acid in acetonitrile (solvent B) at a flow rate of 0.35 mL/min. 4 μL of each sample was injected after equilibration. The gradient program was as follows: 5 % B (0–9 min), from 5 to 95 % B (9–10 min), 95 % B (10–11 min), from 95 to 5 % B (11–11.1 min), and 5 % B (11.1–14 min).

The MS/MS data were acquired on AB SCIEX QTRAP 4500 System equipped with linear ion trap (LIT) and triple quadrupole (QQQ) scans.

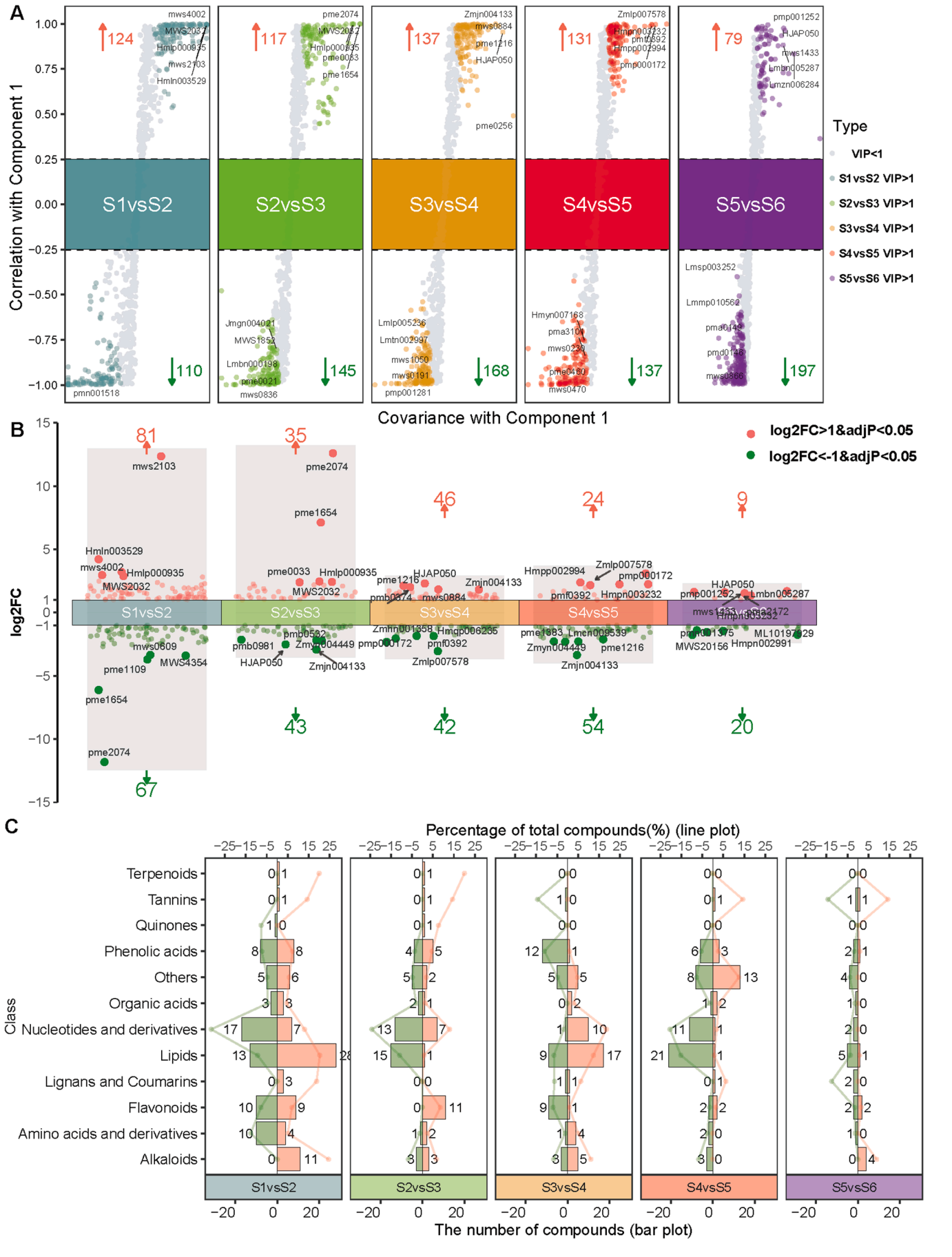

(caption on next page)

Fig. 3. Differences in the metabolites during *Dioscorea opposita* Thunb. cv. Tiegun harvest stages between S1 vs S2, S2 vs S3, S3 vs S4, S4 vs S5 and S5 vs S6. VIP S-plots of OPLS-DA analysis during harvest stages. The gray color showed the VIP < 1, and the other color showed the VIP > 1 (A). Differential metabolites analysis showing up- and down-regulated metabolites at harvest stages. The log2 FC > 1 and adjusted p value < 0.05 was indicated in red, while log2 FC < -1 and adjusted p value < 0.05 was indicated in green (B). The quantities of up and down regulated metabolites and their proportions of total terpenoids, alkaloids, amino acids and derivatives, flavonoids, lignans and coumarins, lipids, nucleotides and derivatives, organic acids, phenolic acids, quinones, tannins, and others (C).

The optimal parameters were described as follow: source temperature, 550 °C; ion spray voltage, 5500 V (positive ion mode) and −4500 V (negative ion mode); gas I, gas II and curtain gas as 50, 60, and 25 psi, respectively; collision-activated dissociation was set to high. Instrument tuning and mass calibration were respectively carried out with 10 and 100 μmol/L of polypropylene glycol solutions in QQQ and LIT scan modes. The MS data were acquired both in positive and negative ionization modes. Data acquisition and processing were carried out using Analyst software (version 1.7; AB Sciex, USA) (Liu, Xiao, Wang, Wang & Xu, 2021). Metabolite identification was performed utilizing the MWDB database (Metware, Wuhan, China) in conjunction with several public metabolites databases such as HMDB (https://www.hmdb.ca/), PubChem (https://pubchem.ncbi.nlm.nih.gov/) and MassBank (https://www.massbank.jp/).

2.4. Statistical analysis

Data analysis was performed using R software packages (https://www.r-project.org/). Principal component analysis (PCA), using the "PCAtools" package, was conducted to visualize the sample clustering at six harvest periods. Orthogonal partial least-squares discriminant analysis (OPLS-DA) was performed to screen the differential metabolites using the "ropls" packages. Prior to the OPLS-DA model, the dataset was log-transformed, mean-centered, and pareto-scaled. Firstly, 200 times permutation test was carried out to ascertain if the OPLS-DA model was overfitted. Then, metabolites contributing significantly to the separation of different groups were selected based on a variable importance in the projection (VIP) value (VIP >1), fold change (FC) value ($|\log2(FC)| > 1$), and an adjust p-value ($p < 0.05$). Subsequently, the calculations of correlation (cor) and covariance (cov) in the OPLS-DA model were performed with the " cor " and " cov " functions in R, which further verified screened metabolites. Finally, differential metabolites were determined based on these screening criteria. The Kyoto Encyclopedia of Genes and Genomes (KEGG) database was further used to analyze and annotate the metabolic pathways of these differential metabolites.

3. Results

3.1. Metabolites identification of Dioscorea opposita thunb. Cv. Tiegun

To elucidate the distinct metabolic changes during harvest, we collected samples from six different stages during harvest (Fig. 1A) and analyzed their metabolic profiles. In total, 767 metabolites were identified by LC-MS including 138 lipids, 129 flavonoids, 109 phenolic acids, 79 amino acids and derivatives, 67 organic acids, 54 nucleotides and derivatives, 45 alkaloids, 16 lignans and coumarins, 13 quinones, 7 tannins, 5 terpenoids, 1 steroids and 104 others (Table S1). Among them, lipids (17.99 %), flavonoids (16.82 %), phenolic acids (14.21 %), amino acids and derivatives (10.30 %) and organic acids (8.74 %) were the main metabolites in *Dioscorea opposita* thunb. cv. Tiegun (Fig. 1B).

3.2. Multivariate statistical analysis to screen differential metabolites

Initially, PCA, an unsupervised multivariate statistical analysis method, was utilized to analyze the overall differences of *Dioscorea opposita* thumb. cv. Tiegun. As shown in Fig. 2, the PCA score plot showed the changing trends of samples during six different harvest stages. It could be clearly seen that it was divided into two large groups, namely S1-S3 group and S4-S6 group. The result also showed that the metabolites in *Dioscorea opposita* thumb. cv. Tiegun had greatly changes from S1 to S2, S2 to S3 and S3 to S4, and the discrepancy was diminished from S4 to S5 and S5 to S6. Moreover, the QC samples displayed high clustering, indicating the method had good stability and repeatability. Total ion chromatography (TIC) overlap diagrams of QC samples in positive and negative modes also revealed the reliability of the data (Fig. S1). To clarify the changes in metabolites between different harvest stages, OPLS-DA models of S1 vs S2, S2 vs S3, S3 vs S4, S4 vs S5 and S5 vs S6 were further performed to screen the differential metabolites with VIP value > 1, log2(FC) > 1 or log2(FC) < −1 and adjust p value < 0.05. Based on these criteria, we identified 148, 78, 88, 78, and 29 potential differential metabolites for each respective pair of harvest stages (Fig. 3A and B). Result revealed that substantial fluctuations in metabolite levels during S1, S2 and S3 stages, and minimal alterations during S4, S5 and S6 stages. These findings suggested that the metabolites might be mainly engaged in synthesis and accumulation processes during the initial three harvest periods, whereas the metabolic activity appeared to stabilize during the final three harvest periods. Furthermore, the bar plot and line plot depicted the number and the percentage of total compounds within various types of metabolites, respectively (Fig. 3C). The results demonstrated that the metabolite alterations during the three stages of S1, S2 and S3 were more substantial in terms of type, quantity and range compared with stages S4, S5 and S6, which indicated that the relative content and dynamic trend of differential metabolites were closely related to the harvesting period. Interestingly, our study also found a higher number of metabolite changes between S3 and S4 compared to S2 and S3, but the extent of these changes remained relatively modest. The detail information on the up-regulated (Fig. S2A) or down-regulated (Fig. S2B) of compounds was also shown in heatmap. Notably, the harvest time of S1, S2, and S3 occur before frost, whereas S4, S5, and S6 occur after frost. This phenomenon also indicated that frost may be a significant impact on the changes in metabolites, and the changes of metabolites tend to stabilize basically after frost.

Subsequently, the six different harvest stages were divided into two distinct groups, namely S1-S3 group and S4-S6 group. OPLS-DA model was performed to determine the differential metabolites of the two new groups. The score plot of OPLS-DA exhibited clear differentiation between the samples of S1-S3 group and S4-S6 group (Fig. 4A). With R^2X and Q^2 values of 0.512 and 0.977, the stability and robustness of the OPLS-DA model were confirmed by permutation test (Fig. 4B). Differential metabolites were detected on the basis of two analyses including the volcano plots and S-plot. In the volcano plots, these metabolites were selected based on the following principles

VIP value >1 (Fig. 4C), fold change value >2 or <0.5 and adjust p value <0.05 (Fig. 4D). Consequently, 38 metabolites were screened and presented in Venn diagram (Fig. 4E). In addition, the S-plot of OPLS-DA also obtained 38 differential metabolites by their covariance and correlation (Fig. 4F), which validated the results of the volcano plots. Among these 38 metabolites, 22 metabolites were found to be more abundant in the S4-S6 group, suggesting an increased presence during the late harvest stages. Conversely, the remaining metabolites were more prevalent in S1-S3 group, indicating higher levels during early harvest stage. The violin charts further clearly depicted the differences of 38 differential metabolites. As demonstrated in Fig. 5A, the up-regulated metabolites included 4 alkaloids, 4 amino acids and derivatives, 4 flavonoids, 1 organic acid, 1 phenolic acid, 1 tannin, and 7 others. Among these, the up-regulated flavonoids, such as catechin, epicatechin, fustin, and mearnsetin-3-O-glucoside, comprised the entire set of identified flavonoids. Up-regulated amino acids and derivatives,

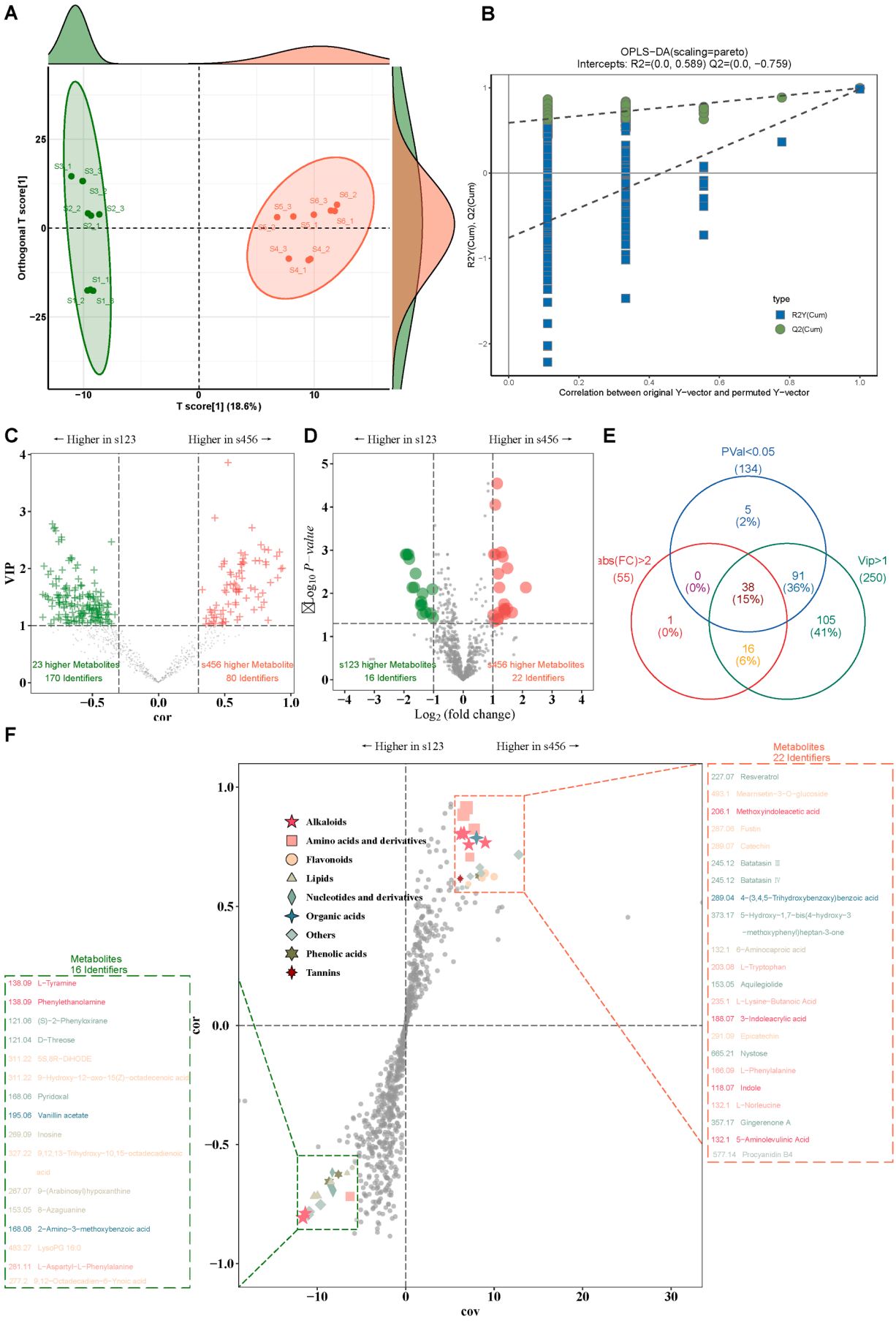

(caption on next page)

Fig. 4. Multivariate analysis of *Dioscorea opposita* Thunb. cv. Tiegun samples from S1-3 and S4-6 groups. OPLS-DA score plot of S1-3 and S4-6 samples (A). Cross-validation plot with 200 times permutation test (B). V-plot of OPLS-DA model, the red and green points represented metabolites with VIP > 1, while the gray points represented metabolites with VIP < 1 (C). Volcano plot of OPLS-DA model. The data points located in the upper right corner (log2FC > 1 and ajust P<0.05) in green and upper left corner in red (log2FC < -1 and ajust P<0.05), signifying metabolites that exhibited significant differences between the two groups (D). Venn diagram of differential metabolites (E). S-plot of metabolite changes responsible for S1-3 and S4-6 separation (F).

including L-lysine-butanoic acid, L-norleucine, L-phenylalanine, and L-tryptophan, constituted 80 % of all identified amino acids and derivatives. Up-regulated alkaloids, such as 3-indoleacrylic acid, 5-aminolevulinic acid, indole, and METHOA, accounted for 67 % of all identified alkaloids. Furthermore, secondary metabolites like batatasin III, batatasin IV, gingerenone A, and resveratrol exhibited an accumulation trend. As described in Fig. 5B, down-regulated metabolites consisted of 2 alkaloids, 1 amino acid and derivative, 5 lipids, 3 nucleotides and derivatives, 2 phenolic acids, and 3 others. Among these, down-regulated lipids, including 5S, 8R-DiHODE, 9-H-12-O-ONA, 9, 12-octad-6-YA, 9, 12, 13-TriHONA, and Lyso PG 16:0, and down-regulated nucleotides and derivatives, such as 8-Azaguanine, 9(Arab)hypoxanthine, and inosine, encompassed all identified lipids and nucleotides and derivatives, respectively.

3.3. Metabolic pathway enrichment analysis

To comprehend the influence of harvest time on metabolite accumulation, the relevant enrichment pathways of 38 screened differential metabolites were obtained by KEGG database. Fig. 6 displayed the bubble plots, which presented the relative variation abundance of each differential metabolite and enrichment pathways. The left bubble plots showed the trends of 38 metabolites changes from S1 to S6. During harvest stages, 22 metabolites exhibited a primarily increasing trend, while 16 metabolites revealed a decreasing trend, which accorded with the result of the violin chart. The right histogram indicated that the differences in metabolites during the harvest period were primarily enriched in 26 metabolic pathways. Among them, phenylalanine, tyrosine and tryptophan biosynthesis (p value = 0.02 and rich factor = 0.11), stilbenoid, diarylheptanoid and gingerol biosynthesis (p value = 0.03 and rich factor = 0.08), phenylpropanoid biosynthesis (p value = 0.04 and rich factor = 0.07), flavonoid biosynthesis (p value = 0.04 and rich factor = 0.07) and tryptophan metabolism (p value = 0.04 and rich factor = 0.06) were considered as the main major pathways. Interestingly, three of the five major metabolic pathways were directly related to the synthesis of secondary metabolites, including stilbenoid, diarylheptanoid and gingerol biosynthesis, phenylpropanoid biosynthesis and flavonoid biosynthesis. Previous studies have shown that low temperature stress can effectively promote the accumulation of secondary metabolites and play an important role in regulating secondary metabolites and improving plant cold resistance (Thakur, Bhattacharya, Khosla & Puri, 2019; Gao, Zhang, Lv, Cheng, Peng & Cao, 2016). In response to cold stress, plants usually synthesize more phenolic acids and flavonoids, thereby enhancing the thickness of cell walls and helping to prevent chilling injury and cell collapse under cold stress (Zhou, et al., 2018; Naikoo, et al., 2019; Sharma, Shahzad, Rehman, Bhardwaj, Landi & Zheng, 2019; Pant, Pandey & Dall'Acqua, 2021). It is worth noting that the S4, S5 and S6 harvesting periods of yam occurred after frost. The temperature during this period dropped sharply, causing the secondary metabolite synthesis pathway in yam to be more active. This finding more reasonably explained the increase in secondary metabolites in yam after frost.

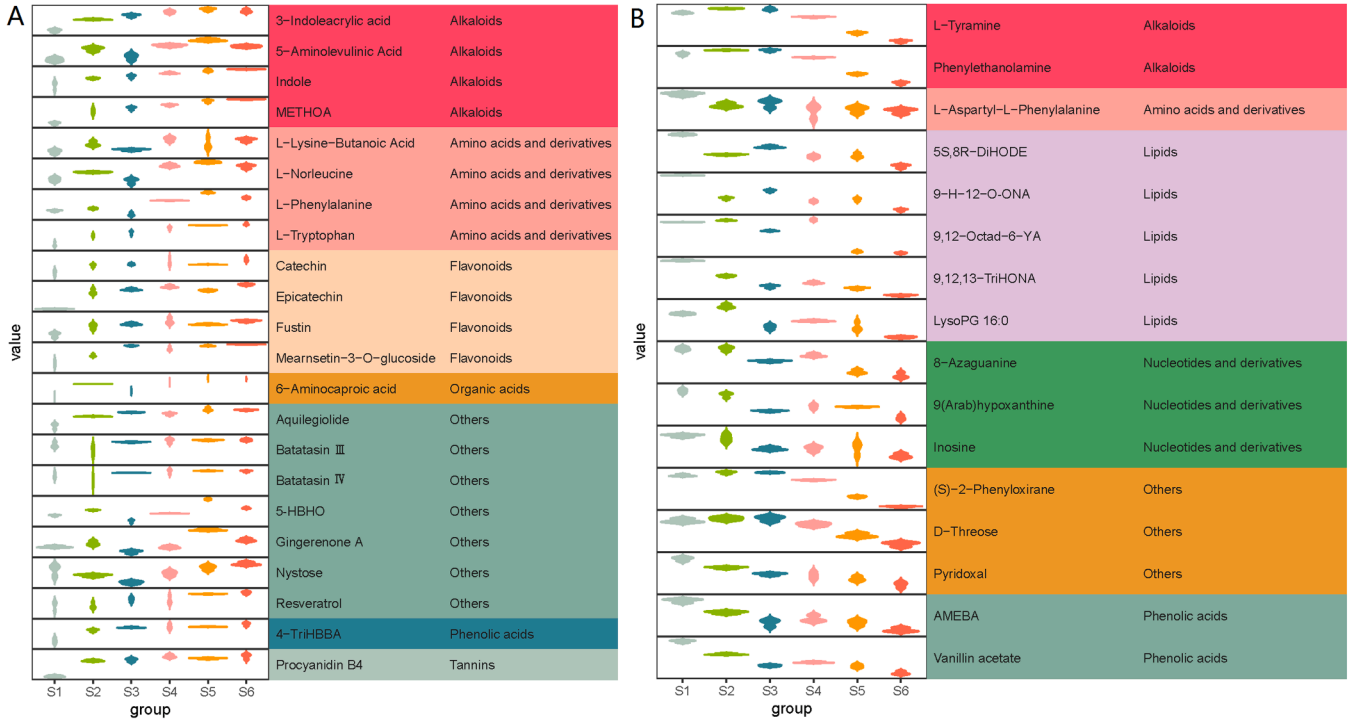

Fig. 5. The violin plot of differential metabolite changes. Up-regulated metabolites (A) and down-regulated metabolites (B). Abbreviations: 4-TriHBBA, 4-(3, 4, 5-Trihydroxybenzoxy) benzoic acid; 5-HBHO, 5-Hydroxy-1, 7-bis(4-hydroxy-3-methoxyphenyl)heptan-3-one; 5S, 8R- DiHODE, (5S, 8R, 9Z, 12Z) -5, 8-Dihydroxyoctadeca-9, 12-dienoate; 9, 12, 13-TriHONA, 9, 12, 13-Trihydroxy-10, 15-octadecadienoic acid ; 9, 12-Octa-6-YA, 9, 12-Octade cadien-6-Ynoic Acid; 9-(Arab)hypoxanthine, 9-(Arabinosyl) hypoxanthine; 9-H-12-O-ONA, 9-Hydroxy-12-oxo-15(Z)-octadecenoic acid; AMEBA, 2-Amino-3 -methoxybenzoic acid; METHOA, Methoxyindoleacetic acid.

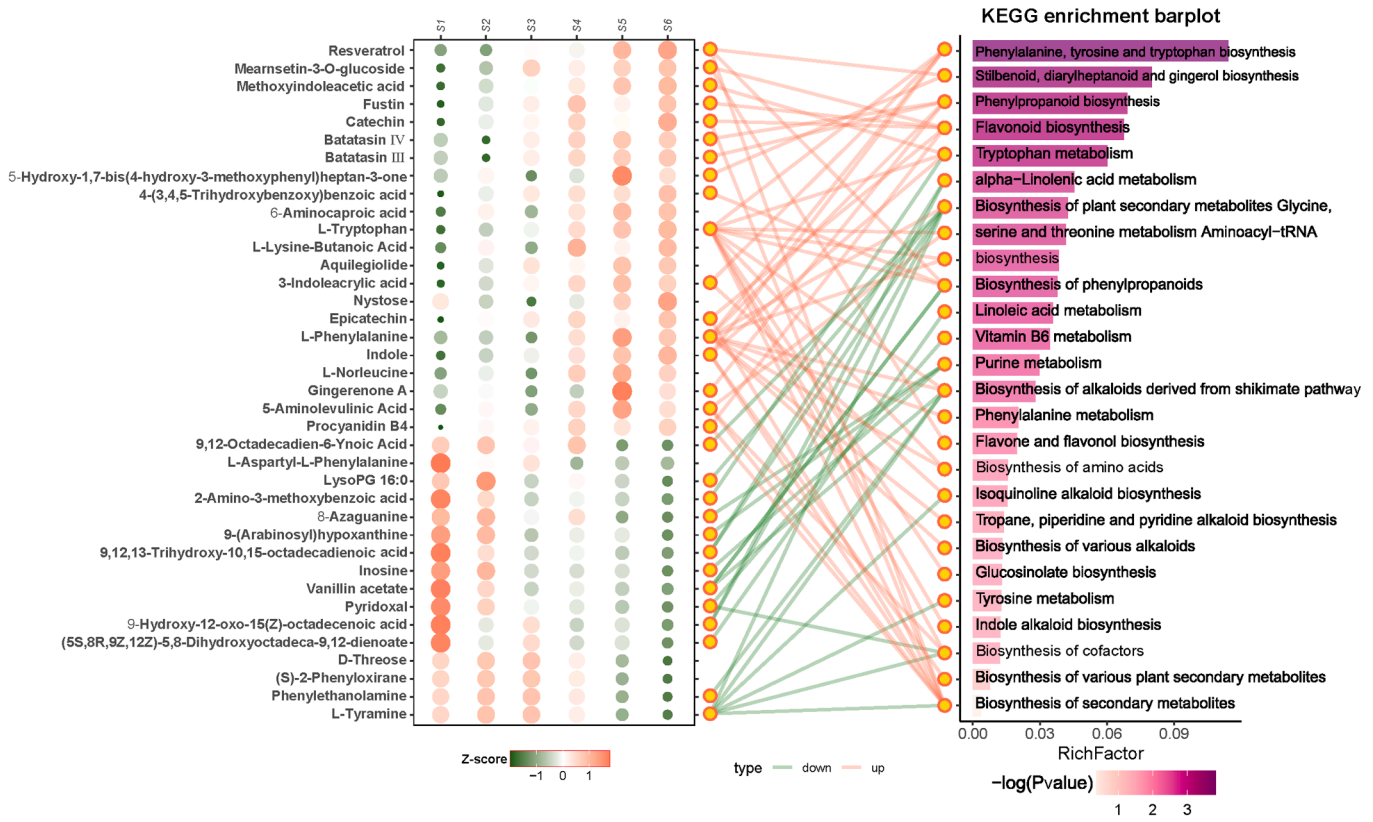

Fig. 6. Changes in the levels of differential metabolites during harvest of *Dioscorea opposita* Thunb. cv. Tiegun, and the red (or green) ball represented up-regulated (or down-regulated) metabolites in S1-S6 samples. KEGG pathway enrichment analyses identified significantly enriched metabolic pathways, and the red (or green) line connected the metabolic pathway of up-regulated (or down-regulated) metabolites in S1-S6 samples.

4. Discussion

Harvest time plays an important role in the accumulation of metabolites, especially for medicinal and edible homologous plants. Secondary compounds in medicinal plants possess biological activities, which can improve human health in the pharmaceutical and food industries (Rasool Hassan, 2012). Currently, although the metabolites biosynthesis and accumulation research are progressed, the reports on the effect of different harvest time on the synthesis and accumulation of metabolites still rarely. Due to the obvious difference in the life cycle of different plants, a substantial amount of active compounds often occurs at a certain stage of plant growth. Therefore, it is necessary to investigate the optimal harvest period for medicinal and edible homologous plants. In this study, widely targeted metabolomics approach was firstly applied to identify the variations in metabolites during six different harvest stages of *Dioscorea opposita* thumb. cv. Tiegun and explore the suitable harvest time. The periods of S1, S2, and S3 occur before frost, while S4, S5, and S6 occur after frost. The result revealed 38 metabolites had significant changes, 22 of which exhibited up-regulated, while 16 metabolites showed down-regulated. KEGG enrichment analysis found five significantly enriched metabolic pathways, including phenylalanine, tyrosine and tryptophan biosynthesis, stilbenoid, diarylheptanoid and gingerol biosynthesis, phenylpropanoid biosynthesis, flavonoid biosynthesis and tryptophan metabolism, which indicated that temperature had a potential greater impact on these pathways.

Result indicated that several secondary metabolites, including 4 flavonoids (catechin, epicatechin, fustin and mearnsetin-3-O-glucoside), 4 alkaloids (3-indoleacrylic acid, 5-aminolevulinic acid, indole and METHOA), batatasin III, batatasin IV, gingerenone A, resveratrol and procyanidin B4, were up-regulated during the harvest periods of S4, S5, and S6. Some metabolites have been previously reported to exhibit favorable pharmacological characteristics (Hu, Cao, Zhu, Li & Liu, 2015; Chen et al., 2018; Galiniak, Aebisher & Bartusik-Aebisher, 2019; Jiang, Hong, Mao, Ma, Chen & Wang, 2022; Chen, Chen, Zheng, Zhao, Yu & Zhu, 2022; Kumazoe, Fujimura, Yoshitomi, Shimada & Tachibana, 2022). Secondary metabolites in medicinal and edible homologous plants serve as vital indicators for evaluating medicinal material quality. Root and stem organs in plants are primarily responsible for the accumulation of active components with medicinal value (Li, Kong, Fu, Sussman & Wu, 2020). The growth period of root and stem herbs significantly influences the accumulation of active components (Xu et al., 2014; Hong et al., 2005; Naghiloo, Movafeghi, Delazar, Nazemiyeh, Asnaashari & Dadpour, 2012). Our result indicated that the aboveground parts of *Dioscorea opposita* thumb. cv. Tiegun from S4, S5 and S6 periods gradually wither and turn yellow, and the underground root and stem parts rapid accumulation of active ingredients. The phenomenon was not only closely related to growth, but temperature was also an important factor. During this period (after frost), the temperature begins to decrease and frost occurs. More secondary metabolites with pharmacological effects were produced, which might enhance the resistance of plants to cold stress (Wang, Wu, Guan, Zhao, Geng & Zhao, 2020). Therefore, yams harvested after frost have greater medicinal value and the optimal quality.

Flavonoids, derived from the phenylpropanoid metabolic pathway, assume a crucial role in plant development and defense mechanisms (Buer, Imin & Djordjevic, 2010; Liu et al., 2021). They exhibit a remarkable ability to affect the basic physiological metabolism, stress responses, and disease resistance response in plants. As antioxidants, flavonoids possess the capacity to scavenge reactive oxygen species (Cavaiuolo, Cocetta & Ferrante, 2013), thus safeguarding plants against damage caused by various biotic and abiotic stresses, such as UV irradiation, cold stress and pathogen infection (Zhang et al., 2020). The synthesis of phenylpropanoid metabolites stems from the conversion of phenylalanine, which is derived from the shikimate pathway (Wang,

Wang, Kuang, Hu, Qiao & Ye, 2018). Initially, 4-phosphate erythritol binds with phosphoenol pyruvate (PEP) to produce phenylalanine. Subsequently, phenylalanine undergoes conversion to p-Coumaroyl-CoA, thus entering the phenylpropanoid pathway (Wohl & Petersen, 2020; Barros & Dixon, 2020). Numerous studies have reported an upregulation in the synthesis of secondary metabolites, specifically phenolics and flavonoids, in the phenylpropanoid pathway of plants under abiotic stress conditions. This activation of the phenylpropanoid pathway can promote the accumulation of diverse phenolics and flavonoids, which possess the capability to efficiently scavenge detrimental reactive oxygen species. These findings indicated that such metabolites played a crucial role in aiding plants to cope with environmental constraints (Nagamatsu et al., 2007; Sun et al., 2020; Sun et al., 2021; Wang et al., 2018).

The upregulation of most alkaloids occurred in the S4, S5, and S6 periods. This observation suggested that the higher accumulation of alkaloids might be attributed to the decrease of temperature during the late stages of harvest. Similar studies have reported that the majority of alkaloids exhibit upregulation in response to both biotic and abiotic stresses (Srivastava & Srivastava, 2010). The rapid accumulation of medicinal secondary metabolites not only facilitates the clearance of reactive oxygen species in plants, but also enhances the overall quality and value of medicinal plants. Therefore, it becomes evident that harvest time directly impacts the accumulation of medicinal components.

For lipid metabolites, a decreasing trend was observed in S4-S6 harvest stages including Lyso PG (16:1), 9, 12-Octa-6-YA, (5S, 8R)-DiHODE, 9-H-12-O-ONA and 9, 12, 13-TriHODE. Lipids constitute the primary constituents of cell membranes and perform crucial functions in cellular processes. During the active phase of cell division, which coincides with the growth period of plants, cells exhibit heightened lipid synthesis (Tenenboim, Burgos, Willmitzer & Brotman, 2016). Our findings indicated a decline in the intensity of cell division during the late stages of growth, implying a potential cessation of growth in *Dioscorea opposita* thumb. cv. Tiegun.

In this study, 8-Azaguanine, 9-(Arabinosyl)hypoxanthine and Inosine demonstrated a significant decline at S4, S5, and S6 harvest stages. The plant tissue, known for its high nucleotide content, exhibits a rapid growth rate (Fujisawa, 1966). This result suggested that *Dioscorea opposita* thumb. cv. Tiegun might reach maturity during these stages. Previous studies have found that similar changes in nucleotides and derivatives during growth stages of other plants, such as garlic cloves and asparagus, which were consistent with the findings of our research (Liu et al., 2022; Liu et al., 2020).

5. Conclusion

In this study, a comprehensive widely targeted metabolomics approach was used to determine the metabolic changes during the harvest stages of *Dioscorea opposita* thumb. cv. Tiegun. The results identified 13 secondary metabolites with pharmacological effects, such as 4 flavonoids, 4 alkaloids, batatasin III, batatasin IV, gingerenone A, resveratrol, and procyanidin B4, which exhibited higher levels during the late harvest stages. Pathway analysis revealed that phenylalanine, tyrosine and tryptophan biosynthesis, stilbenoid, diarylheptanoid and gingerol biosynthesis, phenylpropanoid biosynthesis, flavonoid biosynthesis and tryptophan metabolism were active during harvest. Furthermore, our findings also indicated that *Dioscorea opposita* thumb. cv. Tiegun harvested after frost has higher medicinal value. The study was the first to provide critical information for evaluating the quality and confirming the optimal harvest time of *Dioscorea opposita* thumb. cv. Tiegun, which highlighted the potential roles of metabolomics in better understanding of the systematic metabolic changes during harvest and the molecular mechanisms influencing the quality formation.

CRediT authorship contribution statement

Li An: Conceptualization, Data curation, Funding acquisition, Investigation, Visualization, Writing – original draft. **Yongliang Yuan:** Data curation, Formal analysis, Software, Visualization, Writing – review & editing. **He Chen:** Formal analysis, Investigation, Writing – review & editing. **Meng Li:** Formal analysis, Investigation, Methodology. **Jingwei Ma:** Formal analysis, Writing – original draft. **Juan Zhou:** Formal analysis, Validation. **Lufei Zheng:** Conceptualization, Methodology. **Huan Ma:** Formal analysis, Validation. **Zenglong Chen:** Funding acquisition, Investigation, Supervision, Writing – review & editing. **Chenyu Hao:** Formal analysis, Validation. **Xujin Wu:** Funding acquisition, Investigation, Resources, Supervision, Writing – review & editing.

Declaration of competing interest

The authors declare that they have no known competing financial interests or personal relationships that could have appeared to influence the work reported in this paper.

Data availability

Data will be made available on request.

Acknowledgments

This work was supported by the Central Plains Science and Technology Innovation Leading Talent Project (234200510012), the Scientific-Technological Innovation of Henan Academy of Agricultural Sciences (2023TD18), the Independence Innovation Projects of Henan Academy of Agricultural Sciences (2023ZC073), and the National Natural Science Foundation of China (31801771).

Appendix A. Supplementary data

Supplementary data to this article can be found online at https://doi.org/10.1016/j.fochx.2024.101159.

References

Barros, J., & Dixon, R. A. (2020). Plant phenylalanine/tyrosine ammonia-lyases. *Trends in Plant Science, 25*, 66–79. https://doi.org/10.1016/j.tplants.2019.09.011

Buer, C. S., Imin, N., & Djordjevic, M. A. (2010). Flavonoids: New roles for old molecules. *Journal of Integrative Plant Biology, 52*, 98–111. https://doi.org/10.1111/j.1744-7909.2010.00905.x

Cavaiuolo, M., Cocetta, G., & Ferrante, A. (2013). The antioxidants changes in ornamental flowers during development and senescence. *Antioxidants, 2*, 132–155. https://doi.org/10.3390/antiox2030132

Chen, J., Chen, Y., Zheng, Y., Zhao, J., Yu, H., & Zhu, J. (2022). Relationship between neuroprotective effects and structure of procyanidins. *Molecules, 27*, 2308. https://doi.org/10.3390/molecules27072308

Chen, J., Sun, J., Prinz, R. A., Li, Y., & Xu, X. (2018). Gingerenone A sensitizes the insulin receptor and increases glucose uptake by inhibiting the activity of p70 S6 kinase. *Molecular Nutrition & Food Research, 62*, 1800709. https://doi.org/10.1002/mnfr.201800709

Deiana, P., Santona, M., Dettori, S., Culeddu, N., Dore, A., & Molinu, M. G. (2019). Multivariate approach to assess the chemical composition of Italian virgin olive oils as a function of variety and harvest period. *Food Chemistry, 300*, Article 125243. https://doi.org/10.1016/j.foodchem.2019.125243

Epping, J., & Laibach, N. (2020). An underutilized orphan tuber crop—Chinese yam: A review. *Planta, 252*, 58. https://doi.org/10.1007/s00425-020-03458-3

Fujisawa, H. (1966). Role of nucleic acid and protein metabolism in the initiation of growth at germination. *Plant and Cell Physiology, 7*, 185–197. https://doi.org/10.1093/oxfordjournals.pcp.a079173

Galiniak, S., Aebisher, D., & Bartusik-Aebisher, D. (2019). Health benefits of resveratrol administration. *Acta Biochimica Polonica, 66*, 13–21. https://doi.org/10.18388/abp.2018_2749

Gao, H., Zhang, Z., Lv, X., Cheng, N., Peng, B., & Cao, W. (2016). Effect of 24-epibrassinolide on chilling injury of peach fruit in relation to phenolic and proline metabolisms. *Postharvest Biology and Technology, 111*, 390–397. https://doi.org/10.1016/j.postharvbio.2015.07.031

Hong, D., Lau, A., Yeo, C., Liu, X., Yang, C., Koh, H. L., & Hong, Y. (2005). Genetic diversity and variation of saponin contents in Panax notoginseng roots from a single

farm. *Journal of Agricultural and Food Chemistry, 53*, 8460–8467. https://doi.org/10.1021/jf051248g

Hu, W., Cao, G., Zhu, J., Li, J., & Liu, X. (2015). Naturally occurring Batatasins and their derivatives as α-glucosidase inhibitors. *RSC Advances, 5*, 82153–82158. https://doi.org/10.1039/c5ra15328j

Jiang, M., Hong, K., Mao, Y., Ma, H., Chen, T., & Wang, Z. (2022). Natural 5-Aminolevulinic Acid: Sources, Biosynthesis, Detection and Applications. *Frontiers in bioengineering and biotechnology, 10*, Article 841443. https://doi.org/10.3389/fbioe.2022.841443

Kawasaki, M., Kanehira, S., & Islam, M. N. (2014). Effects of the direction of gravistimulation on tuber formation and amyloplast distribution in tuber tips of Chinese yam. *Plant Production Science, 17*, 298–304. https://doi.org/10.1626/pps.17.298

Kumazoe, M., Fujimura, Y., Yoshitomi, R., Shimada, Y., & Tachibana, H. (2022). Fustin, a Flavanonol, Synergically Potentiates the Anticancer Effect of Green Tea Catechin Epigallocatechin-3-O-Gallate with Activation of the eNOS/cGMP Axis. *Journal of Agricultural and Food Chemistry, 70*, 3458–3466. https://doi.org/10.1021/acs.jafc.1c07567

Li, Y., Ji, S., Xu, T., Zhong, Y., Xu, M., Liu, Y., Li, M., Fan, B., Wang, F., Xiao, J., & Lu, B. (2023). Chinese yam (Dioscorea): Nutritional value, beneficial effects, and food and pharmaceutical applications. *Trends in Food Science & Technology, 134*, 29–40. https://doi.org/10.1016/j.tifs.2023.01.021

Li, Y., Kong, D., Fu, Y., Sussman, M. R., & Wu, H. (2020). The effect of developmental and environmental factors on secondary metabolites in medicinal plants. *Plant Physiology and Biochemistry, 148*, 80–89. https://doi.org/10.1016/j.plaphy.2020.01.006

Liu, P., Gao, R., Gao, L., Bi, J., Jiang, Y., Zhang, X., & Wang, Y. (2022). Distinct Quality Changes of Asparagus during Growth by Widely Targeted Metabolomics Analysis. *Journal of Agricultural and Food Chemistry, 70*, 15999–16009. https://doi.org/10.1021/acs.jafc.2c05743

Liu, P., Weng, R., Xu, Y., Pan, Y., Wang, B., Qian, Y., & Qiu, J. (2020). Distinct quality changes of garlic bulb during growth by metabolomics analysis. *Journal of Agricultural and Food Chemistry, 68*, 5752–5762. https://doi.org/10.1021/acs.jafc.0c01120

Liu, W., Feng, Y., Yu, S., Fan, Z., Li, X., Li, J., & Yin, H. (2021). The flavonoid biosynthesis network in plants. *International Journal of Molecular Sciences, 22*, 12824. https://doi.org/10.3390/ijms222312824

Liu, Y., Xiao, K., Wang, Z., Wang, S., & Xu, F. (2021). Comparison of metabolism substances in Cordyceps sinensis and Cordyceps militaris cultivated with tussah pupa based on LC-MS. *Journal of Food Biochemistry, 45*, e13735.

Nagamatsu, A., Masuta, C., Senda, M., Matsuura, H., Kasai, A., Hong, J. S., Kitamura, K., Abe, J., & Kanazawa, A. (2007). Functional analysis of soybean genes involved in flavonoid biosynthesis by virus-induced gene silencing. *Plant Biotechnology Journal, 5*, 778–790. https://doi.org/10.1111/j.1467-7652.2007.00288.x

Naghiloo, S., Movafeghi, A., Delazar, A., Nazemiyeh, H., Asnaashari, S., & Dadpour, M. R. (2012). Ontogenetic variation of volatiles and antioxidant activity in leaves of Astragalus compactus Lam. *(Fabaceae). EXCLI Journal, 11*, 436. https://doi.org/10.17877/DE290R-4964

Naikoo, M. I., Dar, M. I., Raghib, F., Jaleel, H., Ahmad, B., Raina, A., Khan, F. A., & Naushin, F. (2019). Role and regulation of plants phenolics in abiotic stress tolerance: An overview. *Plant signaling molecules, 157–168*. https://doi.org/10.1016/B978-0-12-816451-8.00009-5

Pant, P., Pandey, S., & Dall'Acqua, S. (2021). The influence of environmental conditions on secondary metabolites in medicinal plants: A literature review. *Chemistry & Biodiversity, 18*, e2100345.

Rasool Hassan, B. A. (2012). Medicinal plants (importance and uses). *Pharmaceut Anal Acta, 3*, 2153–2435. https://doi.org/10.4172/2153-2435.1000e139

Sharma, A., Shahzad, B., Rehman, A., Bhardwaj, R., Landi, M., & Zheng, B. S. (2019). Response of phenylpropanoid pathway and the role of polyphenols in plants under abiotic stress. *Molecules, 24*, 2452. https://doi.org/10.3390/molecules24132452

Si, C., Zeng, D., Yu, Z., Teixeira Da Silva, J. A., Duan, J., He, C., & Zhang, J. (2022). Transcriptomic and metabolomic analyses reveal the main metabolites in Dendrobium officinale leaves during the harvesting period. *Plant Physiology and Biochemistry, 190*, 24–34. https://doi.org/10.1016/j.plaphy.2022.08.026

Srivastava, N. K., & Srivastava, A. K. (2010). Influence of some heavy metals on growth, alkaloid content and composition in Catharanthus roseus L. *Indian Journal of Pharmaceutical Sciences, 72*(6), 775. https://doi.org/10.4103/0250-474X.84592

Sun, J., Qiu, C., Ding, Y., Wang, Y., Sun, L., Fan, K., Gai, Z., Dong, G., Wang, J., & Li, X. (2020). Fulvic acid ameliorates drought stress-induced damage in tea plants by regulating the ascorbate metabolism and flavonoids biosynthesis. *BMC Genomics, 21*, 1–13. https://doi.org/10.1186/s12864-020-06815-4

Sun, S., Fang, J., Lin, M., Hu, C., Qi, X., Chen, J., Zhong, Y., Muhammad, A., Li, Z., & Li, Y. (2021). Comparative metabolomic and transcriptomic studies reveal key metabolism pathways contributing to freezing tolerance under cold stress in kiwifruit. *Frontiers in Plant Science, 747*. https://doi.org/10.3389/fpls.2021.628969

Tenenboim, H., Burgos, A., Willmitzer, L., & Brotman, Y. (2016). Using lipidomics for expanding the knowledge on lipid metabolism in plants. *BIOCHIMIE, 130*, 91–96. https://doi.org/10.1016/j.biochi.2016.06.004

Thakur, M., Bhattacharya, S., Khosla, P. K., & Puri, S. (2019). Improving production of plant secondary metabolites through biotic and abiotic elicitation. *Journal of Applied Research on Medicinal and Aromatic Plants, 12*, 1–12. https://doi.org/10.1016/j.jarmap.2018.11.004

Wang, F., Ren, G., Li, F., Qi, S., Xu, Y., Wang, B., Yang, Y., Ye, Y., Zhou, Q., & Chen, X. (2018). A chalcone synthase gene AeCHS from Abelmoschus esculentus regulates flavonoid accumulation and abiotic stress tolerance in transgenic Arabidopsis. *Acta Physiologiae Plantarum, 40*, 1–13. https://doi.org/10.1007/s11738-018-2680-1

Wang, X., Wu, J., Guan, M., Zhao, C., Geng, P., & Zhao, Q. (2020). Arabidopsis MYB4 plays dual roles in flavonoid biosynthesis. *The Plant Journal, 101*, 637–652. https://doi.org/10.1111/tpj.14570

Wang, Z., Wang, S., Kuang, Y., Hu, Z., Qiao, X., & Ye, M. (2018). A comprehensive review on phytochemistry, pharmacology, and flavonoid biosynthesis of Scutellaria baicalensis. *Pharmaceutical Biology, 56*, 465–484. https://doi.org/10.1080/13880209.2018.1492620

Wohl, J., & Petersen, M. (2020). Functional expression and characterization of cinnamic acid 4-hydroxylase from the hornwort Anthoceros agrestis in Physcomitrella patens. *Plant Cell Reports, 39*, 597–607. https://doi.org/10.1007/s00299-020-02517-z

Xu, C., Tang, T., Chen, R., Liang, C., Liu, X., Wu, C., Yang, Y., Yang, D., & Wu, H. (2014). A comparative study of bioactive secondary metabolite production in diploid and tetraploid Echinacea purpurea (L.) Moench. *Plant Cell, Tissue and Organ Culture, 116*, 323–332. https://doi.org/10.1007/s11240-013-0406-z

Xue, G., Su, S., Yan, P., Shang, J., Wang, J., Yan, C., Li, J., Wang, Q., Xiong, X., & Xu, H. (2022). Integrative analyses of widely targeted metabolomic profiling and derivatization-based LC-MS/MS reveals metabolic changes of Zingiberis Rhizoma and its processed products. *Food Chemistry, 389*, Article 133068. https://doi.org/10.1016/j.foodchem.2022.133068

Zeng, X., Liu, D., & Huang, L. (2021). Metabolome profiling of eight Chinese yam (Dioscorea polystachya Turcz.) varieties reveals metabolite diversity and variety specific uses. *Life, 11*, 687. https://doi.org/10.3390/life11070687

Zhao, J., Li, A., Jin, X., Liangm, G., & Pan, L. (2022). Discrimination of Geographical Origin of Agricultural Products From Small-Scale Districts by Widely Targeted Metabolomics With a Case Study on Pinggu Peach. *Frontiers in Nutrition, 9*, Article 891302.

Zhang, P., Du, H., Wang, J., Pu, Y., Yang, C., Yan, R., Yang, H., Cheng, H., & Yu, D. (2020). Multiplex CRISPR/Cas9-mediated metabolic engineering increases soya bean isoflavone content and resistance to soya bean mosaic virus. *Plant Biotechnology Journal, 18*, 1384–1395. https://doi.org/10.1111/pbi.13302

Zhang, Z., Gao, W., Wang, R., & Huang, L. (2014). Changes in main nutrients and medicinal composition of Chinese yam (Dioscorea opposita) tubers during storage. *Journal of Food Science and Technology, 51*, 2535–2543. https://doi.org/10.1007/s13197-012-0776-y

Zhou, J., Fang, T., Li, W., Jiang, Z., Zhou, T., Zhang, L., & Yu, Y. (2022). Widely targeted metabolomics using UPLC-QTRAP-MS/MS reveals chemical changes during the processing of black tea from the cultivar Camellia sinensis (L.) O. Kuntze cv. Huangjinya. *Food Research International*, *162*(Pt B), 112169. https://doi.org/10.1016/j.foodres.2022.112169.

Zhou, P., Li, Q., Liu, G., Xu, N., Yang, Y., Zeng, W., Chen, A., & Wang, S. (2018). Integrated analysis of transcriptomic and metabolomic data reveals critical metabolic pathways involved in polyphenol biosynthesis in *Nicotiana tabacum* under chilling stress. *Functional Plant Biology, 46*, 30–43. https://doi.org/10.1071/FP18099